Effect of prestressed ultrasonic peen forming parameters on bending curvature and spherical deformation of plate

Tao ZHANG[1,2], Lei LI[1], Shi-hong LU[1], Jia-bin ZHANG[1], Zhen ZHOU[1], Hai GONG[2]

1. College of Mechanical and Electrical Engineering,
Nanjing University of Aeronautics and Astronautics, Nanjing 210016, China;
2. State Key Laboratory for High Performance Complex Manufacturing,
Central South University, Changsha 410083, China

Abstract: The elastic prestressed ultrasonic peen forming (UPF) was adopted in order to solve problems of insufficient bending deformation and large spherical deformation of plate during free UPF. The theoretical analysis of prestressed UPF and the influence of elastic prebending moment on deformation were analyzed. Spherical deformation coefficient was defined to quantificationally describe the spherical deformation. Experiments were conducted to compare the differences between free UPF and prestressed UPF processes and the effects of processing parameters on bending curvature and spherical deformation coefficient were studied. The results show that peening trajectory in chordwise direction is beneficial to enlarging spanwise bending deformation and decreasing spherical deformation coefficient. Large prebending curvature is helpful to increase spanwise bending deformation and decrease chordwise deformation, thereby obviously decreasing spherical deformation coefficient. Large spanwise deformation can be obtained under large firing pin velocity, small plate thickness and small offset distance. Large firing pin velocity plays a positive role in decreasing spherical deformation, while plate thickness and offset distance have little effect on it. Above all, prebending curvature and peening trajectory are the most important factors during prestressed UPF process. This study provides guidance for parameters optimization of prestressed UPF for wing plate with large thickness.

Key words: prestressed ultrasonic peen forming; forming curvature radius; spherical deformation coefficient

1 Introduction

Ultrasonic peen forming (UPF) technology with advantages of easy operation, non-pollution, low energy consumption and good comprehensive performance, has been widely used in fields of aerospace, weapons, marine vessels and automobile industry. The intense shock wave generated by ultrasonic generator is transferred to the surface of the metal by impact media of shots or firing pin. UPF is a kind of deformation technology with high energy and high strain rate for its high vibration frequency, strong load effect and quick impact [1]. Large deformation, nanostructured surface layer and residual comprehensive stress can be generated on the surface of the metal, which remarkably improve mechanical properties, fatigue life and corrosion resistance [2−4].

The study on UPF process is mainly focused on the bending deformation, residual stress and properties of the metal plate. As the UPF process and the effect of processing parameters on the variation of deformation and residual stress is quite complex, numerical simulation models are widely used. GARIEPY et al [5] established a finite element model (FEM) to study the effect of peening trajectory on deformation of the plate during UPF process. The relationship between shot impact velocity and crater depth was studied in Rousseau's model [6], while the relationship between shot impact angles and impact density of the plate was studied in Badreddine's model [7]. LU et al [8,9] studied the stability of plate for different impact amplitudes during UPF process and analyzed the influence of the

thickness and width of strengthening ring on the curvature radius difference. For surface morphology, YIN et al [10] studied the effects of shot diameter and shot peening time on the surface morphology, and MAREAU et al [11] studied the effects of ultrasonic shot peening (USP) parameters on roughness for stainless steel. For residual stress, CHAISE et al [12] established models to predict distortions and residual stresses induced by UPF. GUO et al [13] studied the influence of the second impact on the residual stress variation induced by the first impact. FAN and ZHAO [14] analyzed the effects of treated material, diameter of shots and peening velocity on the value and depth of residual stress. Moreover, many researches [15−17] had been conducted on the effect of process parameters of USP on surface nanocrystallization. UPF process was known to improve the fatigue life for different materials, and KAKIUCHI et al [18] conducted experiment to study high cycle fatigue behavior of 304 stainless steel after UPF. DONG et al [19] studied the effect of UPF on corrosion of ferritic–martensitic steels. Prestressed UPF had been investigated by many researchers. XIAO et al [20,21] simulated the effect of prestress on the variation of stress distribution after UPF. MIAO et al [22] experimentally studied the effects of peening time and peening velocity on the residual stress as well as the effect of prebending moment on the arc length. HU et al [23] combined eigenstrain-based model and experiments to study the influence of prestress on the bending deformation and residual stress of aluminum alloy 2024-T351 during laser peen forming.

However, the theoretical analysis of prestressed UPF was rarely carried out. Furthermore, prestressed UPF is known to enlarge bending deformation even for thick plate and decrease spherical deformation. The effects of processing parameters on deformation enlargement and spherical deformation decrease need to be further studied to acquire optimized forming parameters. In this work, theoretical model of prestressed UPF was established and the variations of forming curvature in spanwise and chordwise directions were analyzed. Prestressed UPF experiments were conducted to study the effects of processing parameters (peening trajectory, prebending curvature, firing pin velocity, plate thickness and offset distance) on variations of forming curvature and spherical deformation. This study can provide guideline for the optimization of processing parameters and development of prestressed UPF technology for wing plate with large thickness.

2 Theoretical analysis

During prestressed UPF, elastic bending moment is applied to the plate before peening. The tensile stress on

the surface induced by the bending moment is beneficial to the appearance of extensional deformation of the plate. The theoretical analysis of prestressed UPF process is shown in Fig. 1.
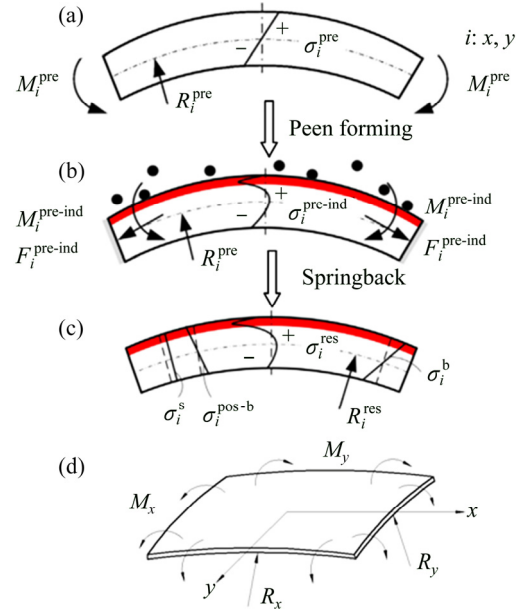

Fig. 1 Schematic diagrams for theoretical analysis of prestressed UPF: (a) Prebending process; (b) Peening process; (c) Springback process; (d) Bending curvature after prestressed UPF

It is assumed that elastic prebending moment through the x direction (spanwise direction) M_x^{pre} is applied on the unit width of the plate and corresponding stress σ_x^{pre} is induced. The prebending moment through the y direction (chordwise direction) is neglected, as shown in Fig. 1(a). In the process of shot peening, the upper surface of the plate is impacted by the firing pin. As a result, severe plastic deformation and induced stress $\sigma_i^{\text{pre-ind}}$ are produced on the upper surface. This induced stress destroys the existing stress balance inside the plate, as shown in Fig. 1(b). After shot peening, stretching force F_i^{ind} and induced bending moment M_i^{ind} are produced on the unit width of the plate under the action of $\sigma_i^{\text{pre-ind}}$ before removing the constraint conditions. After removing the constraint conditions, the balance of internal stresses is achieved again by occurrence of bending deformation. The stretching force and prebending moment turn into $F_i^{\text{pre-ind}}$ and $M_i^{\text{pre-ind}}$, as shown in Fig. 1(c). The effect of $F_i^{\text{pre-ind}}$ on forming curvature is neglected. The forming curvature radius on bending direction (R_x) and that perpendicular to bending direction (R_y), as shown in Fig. 1(d), can be calculated by pure bending equations of Eqs. (1) and (2):

$$R_x = \frac{E\left(h - \delta_\varepsilon\right)}{12} \cdot \frac{1}{M_x^{\text{pre-ind}} - \mu M_y^{\text{pre-ind}}} \tag{1}$$

$$R_y = \frac{E(h - \delta_\varepsilon)}{12} \cdot \frac{1}{M_y^{\text{pre-ind}} - \mu M_x^{\text{pre-ind}}} \quad (2)$$

where E is elastic modulus, μ is Poisson ratio, h is thickness of the plate and δ_ε is depth of residual compressive stress after prestressed peening, $M_x^{\text{pre-ind}}$ and $M_y^{\text{pre-ind}}$ are induced bending moments in spanwise and chordwise directions after constraint removal in prestressed UPF, respectively.

Large bending deformation only in one direction is required for many components in airplane, such as the wing panel. Large bending deformation in spanwise direction and small deformation in chordwise direction are beneficial to service life improvement of this sort of component. However, large spherical deformation usually occurs in free UPF, which means that large chordwise deformation will appear in the forming process. In order to quantificationally study the spherical deformation of wall plate during UPF, a spherical deformation coefficient (R_x/R_y) is defined as the ratio of spanwise forming curvature radius to chordwise forming curvature radius, as shown in Fig. 1(d). The value of R_x/R_y being 1 indicates ideal spherical deformation, while the spherical deformation coefficient needs to decrease in actual UPF. The theoretical calculation of spherical deformation coefficient is shown in Eq. (3). As the prebending moment is applied to the x direction of the plate, $M_x^{\text{pre-ind}}$ is larger than $M_y^{\text{pre-ind}}$, the spherical deformation coefficient R_x/R_y is smaller than 1, which indicates that prestressed UPF is beneficial to the decrease of spherical deformation.

$$\frac{R_x}{R_y} = \frac{M_y^{\text{pre-ind}}}{M_x^{\text{pre-ind}}} \cdot \frac{1 - \mu M_x^{\text{pre-ind}}/M_y^{\text{pre-ind}}}{1 - \mu M_y^{\text{pre-ind}}/M_x^{\text{pre-ind}}} \quad (3)$$

The forming curvature radius in spanwise direction (R_x) and that in chordwise direction (R_y) in prestressed state in relation to that in free state (free UPF) (R) are shown in Eqs. (4) and (5), respectively:

$$\frac{R_x}{R} = \frac{1 - \mu}{1 - \mu \dfrac{M_y^{\text{pre-ind}}}{M_x^{\text{pre-ind}}}} \cdot \frac{M^{\text{pre-ind}}}{M_x^{\text{pre-ind}}} \left(\frac{h - \delta_\varepsilon}{h - \delta}\right)^3 \quad (4)$$

$$\frac{R_y}{R} = \frac{1 - \mu}{1 - \mu \dfrac{M_x^{\text{pre-ind}}}{M_y^{\text{pre-ind}}}} \cdot \frac{M^{\text{pre-ind}}}{M_y^{\text{pre-ind}}} \left(\frac{h - \delta_\varepsilon}{h - \delta}\right)^3 \quad (5)$$

where $M^{\text{pre-ind}}$ is induced bending moment after constraint removal in free UPF, and δ is depth of residual compressive stress in free UPF.

The bending moment in y direction in prestressed UPF is nearly equal to that in free state; while bending moment in x direction is much larger than that in the free state as an elastic bending moment is applied before shot peening. Therefore, it can be concluded that

$M_y^{\text{pre-ind}} \approx M^{\text{pre-ind}}$, $R_x < R$ and $R_y > R$.

Based on the theoretical analysis, the forming curvature radius decreases in the bending direction and increases perpendicular to bending direction. The variation range increases with ascending prebending moment. Therefore, prestressed UPF plays a vital role in enhancing bending deformation in prebending direction and decreasing spherical deformation.

3 Experimental

The UPF experiment was conducted by numerical control ultrasonic peening device that consisted of 3-axis CNC machine tool and ultrasonic peening tool. The size of work table was 1400 mm × 650 mm and the rotational speed of spindle was 40−8000 r/min. The ultrasonic peening tool was made up of ultrasonic generator, energy converter, booster, tool heads and firing pin. The diameter of the firing pin was 3 mm and feed velocity of machine tool was 3 m/min. The working frequency was 20 kHz and the maximum amplitude was 50 μm.

In prestressed UPF process, an elastic prebending moment was applied to the plate before ultrasonic peening. The prebending molds with different curvature radii are shown in Fig. 2. The plate was fastened into the curved surface of the prebending molds and different prebending curvatures can be achieved by changing the curvature radii of prebending molds. The tensile stress in the outer layer of the plate should be smaller than the yield strength to ensure that the prebending moment is elastic. However, the elastic deformation turned to plastic deformation after UPF. Combined with von-Mises yield criterion and elastic−plastic theory, the prebending curvature radius should meet the following inequality [23]:

$$R_p \geq \frac{\sqrt{1 - \mu + \mu^2} \cdot Eh}{2(1 - \mu^2)\sigma_s} \quad (6)$$

where R_p is prebending curvature radius, and σ_s is yield strength.
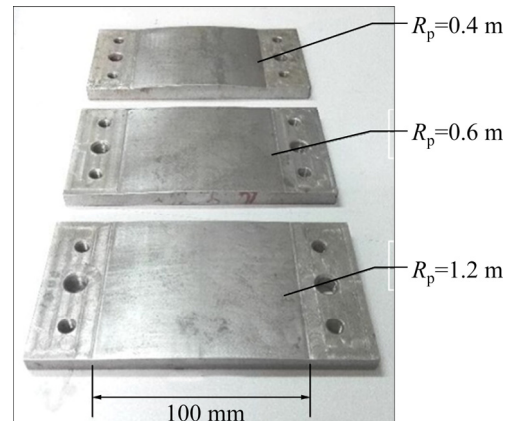

Fig. 2 Prebending molds with different curvature radii R_p

After the UPF process, the forming curvature radii in spanwise and chordwise directions are calculated. The relationship between forming curvature radius and arc height is shown in Eq. (7) [23]. The measurement of arc height is shown in Fig. 3.

$$R=L^2/(8H_{ap}) \tag{7}$$

where H_{ap} is arc height and L is measuring span. The measuring span is 50 mm in chordwise direction and 100 mm in spanwise direction.
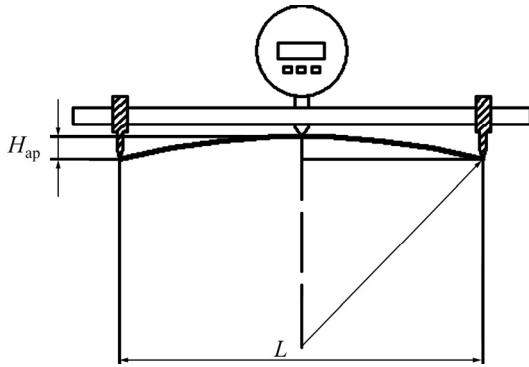

Fig. 3 Relationship between curvature radius and arc height

The experiment material was aluminum alloy 2024-T351 and its size was 120 mm (length) × 50 mm (width). The area of 80 mm × 50 mm in the middle of the plate was set to be ultrasonic peening area. As the UPF process is affected by many factors, the effects of forming parameters (such as peening trajectory, prebending curvature, velocity of firing pin, thickness of plate and offset distance) on forming curvature were studied by variable control method, as shown in Table 1. The variation for velocity of firing pin can be achieved by adjusting the amplitude of the amplitude amplifier, as shown in Eq. (8):

$$v=2\pi Af \tag{8}$$

where v is velocity of firing pin, A and f are amplitude and vibration frequency of the amplifier, respectively.

Table 1 Experimental scheme for UPF process

Experimental parameter	Value
Velocity of firing pin, v/(m·s^{-1})	3, 3.5, 4, 4.5, 5
Offset distance, d/mm	0.6, 0.8, 1.0, 1.2, 1.4
Prebending curvature radius, R_p/m	∞, 1.2, 1.0, 0.8, 0.6, 0.4
Thickness of plate, h/mm	1.5, 2.0, 2.5, 3.0, 3.5

4 Results and discussion

4.1 Peening trajectory

In UPF, the peening trajectory consists of two ways: impact along the spanwise direction (IASD) and impact along the chordwise direction (IACD), as shown in Fig. 4. During forming process of wall plate for aircraft wing, smaller forming curvature radius in spanwise direction (R_x) and larger forming curvature radius in chordwise direction (R_y) are required. Figure 5 shows the effect of peening trajectory on forming curvature radii in spanwise and chordwise directions. With the increase of prebending curvature, spanwise forming curvature radius decreases sharply and then decreases slowly; while chordwise forming curvature radius increases almost linearly for both two shaping trajectories. Furthermore, smaller spanwise forming curvature radius and larger chordwise forming curvature radius are obtained in IACD. Therefore, IACD is beneficial to further enhancing spanwise forming curvature in prestressed UPF.
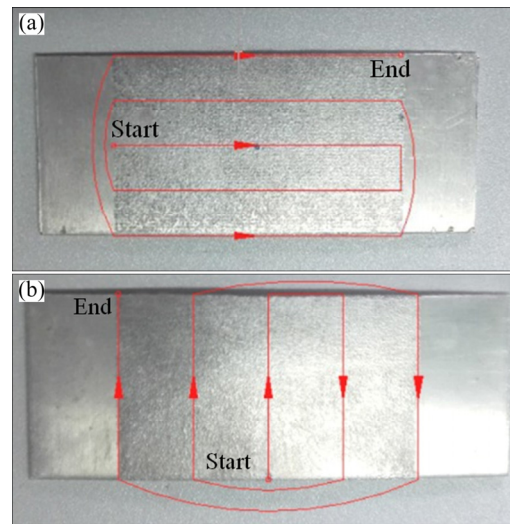

Fig. 4 Schematic diagrams of two shaping trajectories for ultrasonic peen forming: (a) Impact along spanwise direction (IASD); (b) Impact along chordwise direction (IACD)
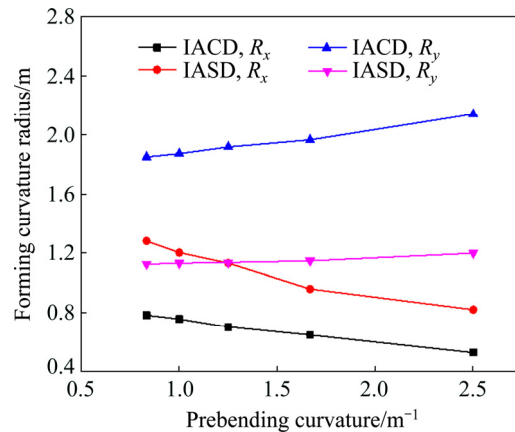

Fig. 5 Effect of peening trajectory on forming curvature radius under conditions of v=4 m/s, d=1.0 mm and h=2.5 mm (R_x refers to spanwise curvature radius and R_y refers to chordwise curvature radius)

The effect of peening trajectory on spherical deformation coefficient is depicted in Fig. 6. The spherical deformation coefficient varies to about 1 at certain value of prebending curvature in IASD; while the spherical deformation coefficient in IACD is always smaller than that in IASD and it decreases with ascending prebending curvature. Based on the above analysis, peening trajectory of IACD is beneficial to enlarging forming curvature in spanwise direction as well as decreasing spherical deformation coefficient in prestressed UPF. Thus, peening trajectory of IACD is adopted in the following experiment for the analysis of other parameters.
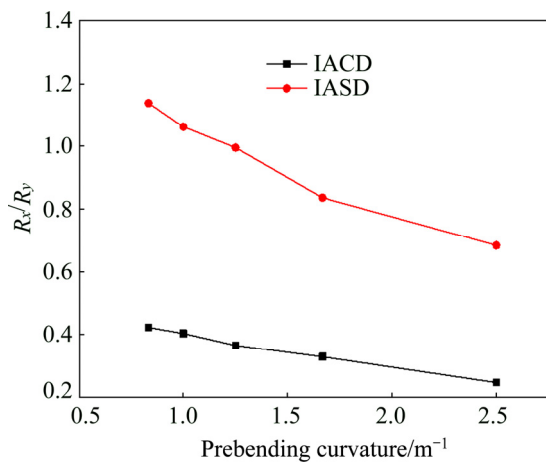

Fig. 6 Effect of peening trajectory on R_x/R_y under conditions of v=4 m/s, d=1.0 mm and h=2.5 mm

4.2 Prebending curvature

Peening trajectory of IACD was adopted and the diagrams of plates with different prebending curvature radii after UPF are shown in Fig. 7. By measuring the values of arc height for different plates, the forming curvature radius can be calculated by Eq. (7). Figure 8 shows the effect of prebending curvature on forming curvature radius in spanwise and chordwise directions. The spanwise curvature radius in prestressed UPF is much smaller than that in free UPF (R_p=∞) as the prebending moment in spanwise direction before peening process contributes greatly to the spanwise bending deformation. While the chordwise forming curvature radius in prestressed UPF is larger, which agrees well with theoretical analysis discussed above. With the increase of prebending curvature, spanwise forming curvature radius sharply decreases first and then decreases slowly, while chordwise forming curvature radius increases almost linearly. When the prebending curvature reaches 2.5 m^{-1} (R_p=0.4 m), a 51.0% reduction in spanwise forming curvature radius and a 26.7% increase in the chordwise forming curvature radius appear compared to free UPF.
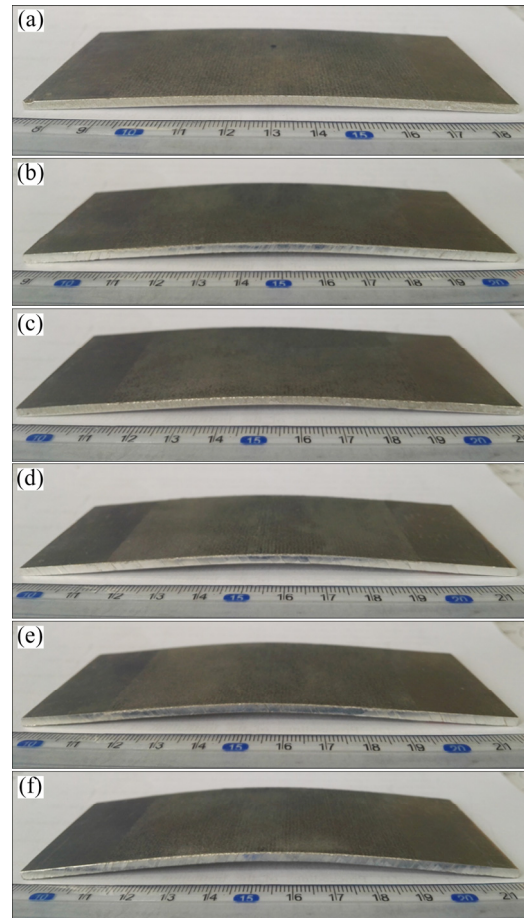

Fig. 7 Diagrams with different prebending curvature radii after UPF under conditions of v=4 m/s, d=1.0 mm and h=2.5 mm: (a) R_p=∞; (b) R_p=1.2 m; (c) R_p=1.0 m; (d) R_p=0.8 m; (e) R_p= 0.6 m; (f) R_p=0.4 m

The effect of prebending curvature on spherical deformation coefficient is depicted in Fig. 6. Large prebending curvature is beneficial to decreasing the spherical deformation coefficient; however, further increase of prebending curvature only has small effect on variation of spherical deformation coefficient. When the prebending curvature increases to a certain value, the induced tensile stress on upper surface of the plate is nearly to its yield limit. At this time, the R_x/R_y nearly reaches its maximum value, the spherical deformation coefficient will not always be decreased as the spanwise forming curvature radius will not reduce to almost zero and the chordwise forming curvature radius will not increase to infinity. As discussed in Eq. (3) in Section 2, the R_x/R_y is concerned with prebending moment through spanwise direction, which will enlarge the value of $M_x^{\text{pre-ind}}$ in Eq. (3) and then decrease the ratio of R_x/R_y. Therefore, prestressed UPF can only reduce the spherical deformation coefficient within a certain range; it cannot achieve the forming of plate with single curvature.
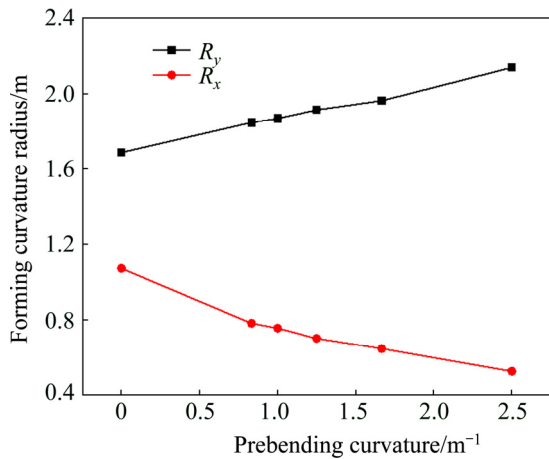
Fig. 8 Effect of prebending curvature on forming curvature radius in IACD peening trajectory under conditions of v=4 m/s, d=1.0 mm and h=2.5 mm

4.3 Velocity of firing pin

During impact process in UPF, the kinetic energy carried by firing pin is transferred to the plate by the strike of firing pin. Elasto−plastic deformation is gradually changed to plastic deformation with increase of firing pin velocity. Figure 9 shows the effect of firing pin velocity on forming curvature radius in spanwise and chordwise directions. Compared to free state, prestressed UPF can drastically reduce the spanwise forming curvature radius especially at small firing pin velocity. Prebending moment is the main factor to enlarge bending deformation at small firing pin velocity in prestressed UPF. However, the difference of spanwise forming curvature radius between two UPF types gradually decreases with ascending firing pin velocity because severe bending deformation will appear at large firing pin velocity for its large kinetic energy. At this time, the role of prebending moment is not so obvious. The spanwise forming curvature radius and the change range both decrease with ascending firing pin velocity. The deformation of the plate may reach its saturated value at a certain firing pin velocity in free state; while it can be further increased with the increase of prebending moment in prestressed UPF. Therefore, the deformation in prestressed state is much larger and it can be further increased. The chordwise forming curvature radius decreases firstly and then increases with ascending firing pin velocity and reaches its minimum value at firing pin velocity of 4 m/s.

The effect of firing pin velocity on spherical deformation coefficient is depicted in Fig. 10. The spherical deformation coefficient decreases with increase of firing pin velocity for free state. The spherical deformation coefficient is much smaller in prestressed state. It reduces to 0.2 at v=5 m/s and R_p=0.4 m. As the bending deformation through spanwise direction can be
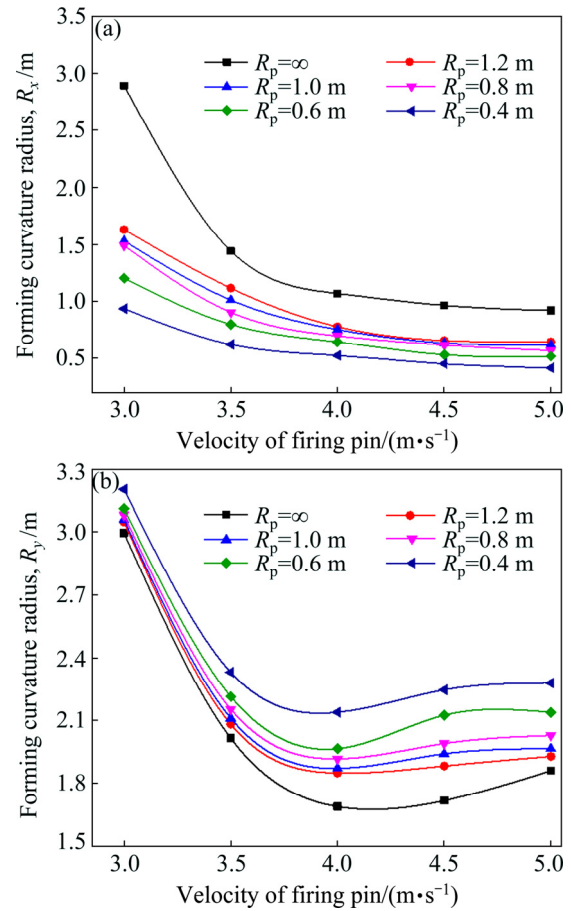

Fig. 9 Effect of firing pin velocity on forming curvature radius in spanwise (a) and chordwise (b) directions in IACD peening trajectory under conditions of d=1.0 mm and h=2.5 mm
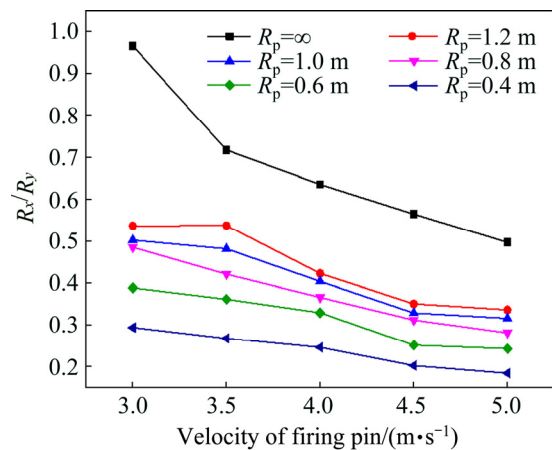

Fig. 10 Effect of firing pin velocity on R_x/R_y in IACD peening trajectory under conditions of d=1.0 mm and h=2.5 mm

further increased with ascending firing pin velocity, the value of R_x is further decreased; therefore, the spherical deformation coefficient can be further decreased at large firing pin velocity for prestressed state. However, large surface roughness will be induced by large firing pin velocity, which will significantly reduce the surface properties of the plate. As discussed above, severe

bending deformation and small spherical deformation can be obtained at large prebending curvature and small firing pin velocity in prestressed UPF, therefore, large prebending curvature and proper firing pin velocity are recommended.

4.4 Thickness of plate

Figure 11 shows the effect of plate thickness on spanwise and chordwise forming curvature radii. The forming curvature radius in spanwise direction increases with ascending plate thickness for both free and prestressed states. However, the change rule is different for two states: the relationship between spanwise forming curvature radius and plate thickness is exponential for free state and it is nearly linear for prestressed state. Bending stress increases with ascending plate thickness, so the bending deformation is much smaller under thick plate. Meanwhile, spanwise forming curvature radius in prestressed state is smaller than that in free state and its difference also increases with ascending plate thickness, which indicates that prestressed UPF is not so sensitive to the variation of plate thickness and it is more efficient to increase bending deformation for thicker plate. In prestressed

UPF, prebending moment and shot peening process both have positive effect on the enlargement of bending deformation through prebending direction as well as deformation depth of the plate. The chordwise forming curvature radius and increasing range increase with ascending plate thickness. As the elastic prebending moment is applied in the spanwise direction of the plate, it results in larger tensile stress than that in chordwise direction, which restricts chordwise deformation for prestressed state.

The effect of plate thickness on spherical deformation coefficient is depicted in Fig. 12. The spherical deformation coefficient increases sharply with ascending plate thickness for free state, which indicates that the degree of spherical deformation after free shot peening is increased for large plate thickness. For prestressed state, there is small fluctuation of the spherical deformation with variation of plate thickness. The spherical deformation coefficient reduces to 0.17 under conditions of R_x=0.4 m and h=3.5 mm, which is quite smaller than that in free state under the same conditions. Meanwhile, with the increase of plate thickness, the spherical deformation coefficient has small decrease in prestressed UPF. Therefore, prestressed UPF can substantially raise the forming curvature as well as restrain spherical deformation for plate with large thickness, which provides guidance for forming process of heavy plate.
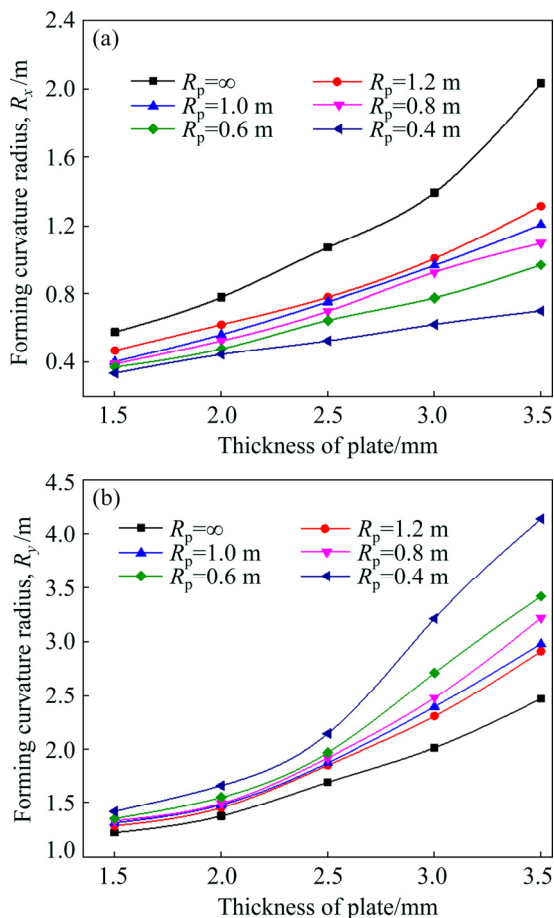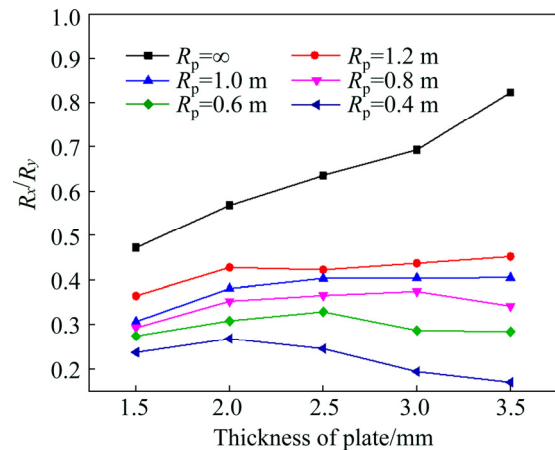

Fig. 11 Effect of plate thickness on forming curvature radius in spanwise (a) and chordwise (b) directions in IACD peening trajectory under conditions of v=4 m/s and d=1.0 mm

Fig. 12 Effect of plate thickness on R_x/R_y in IACD peening trajectory under conditions of v=4 m/s and d=1.0 mm

4.5 Offset distance

The offset distance has a direct effect on the deformation and coverage of the plate during UPF process. The effect of offset distance on forming curvature radius in spanwise and chordwise directions is depicted in Fig. 13. The spanwise forming curvature radius decreases with descending offset distance, which illustrates that small offset distance is beneficial to increasing spanwise bending deformation. With the

decrease of offset distance, the number of impact of firing pin per unit area of the plate is increased. As a result, more impact energy is transferred to the plate and causes larger plastic deformation on the surface of the plate. In prestressed state, the variation tendency is similar to that in free state; while the change rate is smaller compared to free state. However, the effect of offset distance on chordwise forming curvature radius is different between free state and prestressed state. For prestressed state, the chordwise forming curvature radius nearly decreases with descending offset distance and the value of offset distance corresponding to the minimum value of chordwise forming curvature radius also decreases.
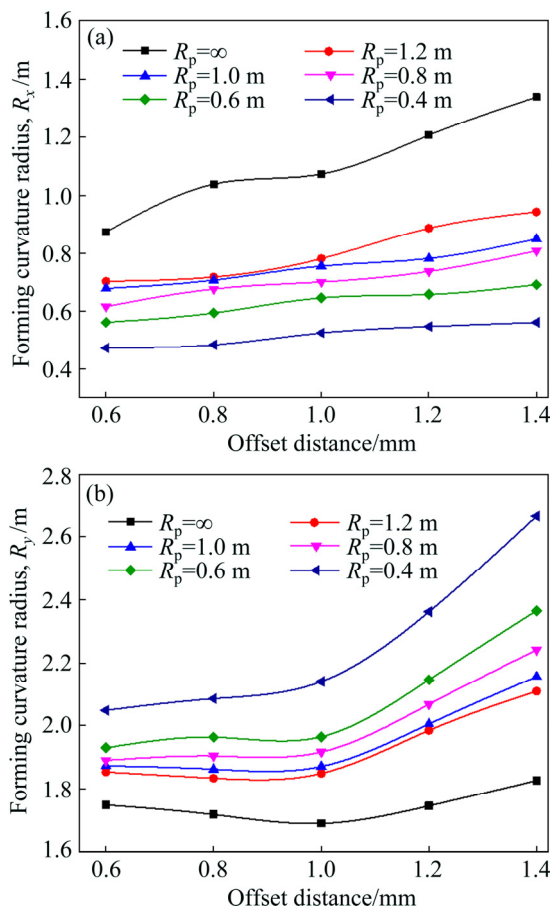

Fig. 13 Effect of offset distance on forming curvature radius in spanwise (a) and chordwise (b) directions in IACD peening trajectory under conditions of v=4 m/s and h=2.5 mm

Figure 14 shows the effect of offset distance on spherical deformation coefficient. The spherical deformation coefficient increases with ascending offset distance for free state, while it is almost unchanged for prestressed state. Offset distance has little effect on the decrease of spherical deformation coefficient; however, prebending curvature significantly changes the spherical deformation coefficient in prestressed UPF. Although small offset distance is beneficial to enlarging bending

deformation, it will decrease the forming efficiency. Therefore, a proper offset distance should be adopted to balance large deformation and forming efficiency.
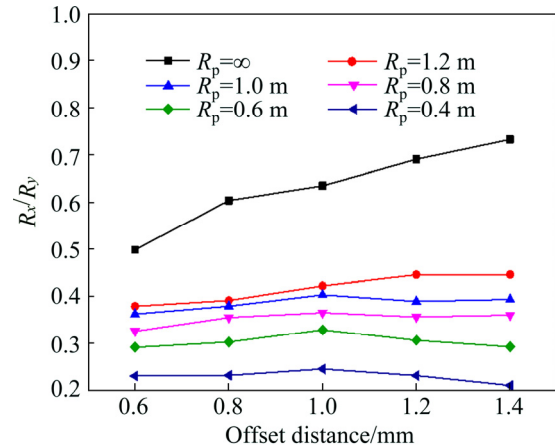

Fig. 14 Effect of offset distance on R_x/R_y in IACD peening trajectory under conditions of v=4 m/s and h=2.5 mm

5 Conclusions

(1) Theoretical analysis of prestressed UPF was conducted and the effect of prebending moment on increase of spanwise bending deformation and decrease of spherical deformation was verified by experiments.

(2) Peening trajectory through the chordwise direction should be adopted in prestressed UPF because it can increase spanwise forming curvature and decrease spherical deformation coefficient.

(3) Large prebending curvature and firing pin velocity are both beneficial to increasing bending deformation of the plate and to decreasing spherical deformation coefficient.

(4) Small plate thickness and offset distance are good for the increase of bending deformation in spanwise direction, while they have little effect on the decrease of spherical deformation.

(5) Prebending curvature is the most important factor in prestressed UPF, which can increase bending deformation for plate with large thickness.

References

[1] SEKKAL A C, LANGLADE C, VANNES A B. A micro/macro impact test at controlled energy for erosion and phase-transformation simulation [J]. Tribology Letters, 2003, 15(3): 265−274.

[2] HE Ya-zhang, WANG Dong-po, WANG Ying, ZHANG Hai. Correction of buckling distortion by ultrasonic shot peening treatment for 5A06 aluminum alloy welded structure [J]. Transactions of Nonferrous Metals Society of China, 2016, 26(6): 1531−1537.

[3] CHEN Guo-qing, JIAO Yan, TIAN Tang-yong, ZHANG Xin-hua, LI Zhi-qiang, ZHOU Wen-long. Effect of wet shot peening on Ti−6Al−4V alloy treated by ceramic beads [J]. Transactions of Nonferrous Metals Society of China, 2014, 24(3): 690−696.

[4] GUJBA A, MEDRAJ M. Laser peening process and its impact on materials properties in comparison with shot peening and ultrasonic impact peening [J]. Materials, 2014, 7(12): 7925−7974.

[5] GARIEPY A, LAROSE S, PERRON C, BOCHER P, LEVESQUE M. On the effect of the peening trajectory in shot peen forming [J]. Finite Elements in Analysis & Design, 2013, 69: 48−61.

[6] ROUSSEAU T, HOC T, GILLES P, NOUGUIER-LEHON C. Effect of bead quantity in ultrasonic shot peening: Surface analysis and numerical simulations [J]. Journal of Materials Processing Technology, 2015, 225: 413−420.

[7] BADREDDINE J, ROUHAUD E, MICOULAUT M, REMY S. Simulation of shot dynamics for ultrasonic shot peening: Effects of process parameters [J]. International Journal of Mechanical Sciences, 2014, 82(5): 179−190.

[8] LU Shi-hong, ZHANG Wei, WU Tian-rui, ZHOU You-liang, ZHOU Zhen. Research on stability of panel ultrasonic peening forming [J]. Key Engineering Materials, 2016, 725: 623−629.

[9] LU Shi-hong, ZHANG Jia-bin, LIU Chao-xun, WU Tian-rui. Ultrasonic peening forming of perforated plate based on thickening design around hole [J]. International Journal of Advanced Manufacturing Technology, 2017, 88(9−12): 2671−2677.

[10] YIN Fei, HUA Lin, WANG Xiao-ming, RAKITA M, HAN Qing-you. Numerical modeling and experimental approach for surface morphology evaluation during ultrasonic shot peening [J]. Computational Materials Science, 2014, 92(5): 28−35.

[11] MAREAU J, BIGERELLE M, MAZERAN P E, BOUVIER S. Relation between roughness and processing conditions of AISI 316L stainless steel treated by ultrasonic shot peening [J]. Tribology International, 2014, 82: 319−329.

[12] CHAISE T, LI Jun, NELIAS D, KUBLERD R, TAHERIB S, DOUCHETC G, VINCET R, GILLESE P. Modelling of multiple impacts for the prediction of distortions and residual stresses induced by ultrasonic shot peening (USP) [J]. Journal of Materials Processing Technology, 2012, 212(10): 2080−2090.

[13] GUO Chao-bo, WANG Zhi-jiang, WANG Dong-po, HU Sheng-sun. Numerical analysis of the residual stress in ultrasonic impact treatment process with single-impact and two-impact models [J]. Applied Surface Science, 2015, 347: 596−601.

[14] FAN Yan-jun, ZHAO Xiao-hui. Research on ultrasonic shot peening through numerical simulation [J]. Applied Mechanics & Materials, 2015, 778: 59−62.

[15] ZHU Li-hua, GUAN Yan-jin, WANG Yan-jie, XIE Zhen-dong, Lin Jun. Influence of process parameters of ultrasonic shot peening on surface nanocrystallization and hardness of pure titanium [J]. International Journal of Advanced Manufacturing Technology, 2017, 89(5−8): 1451−1468.

[16] YIN Fei, HU Shan, HUA Lin, WANG Xiao-ming, SUSLOV S, HAN Qing-you. Surface nanocrystallization and numerical modeling of low carbon steel by means of ultrasonic shot peening [J]. Metallurgical and Materials Transactions A, 2015, 46(3): 1253−1261.

[17] SHENG Xiang-fei, XIA Qin-xiang, CHENG Xiu-quan, LIN lie-shu. Residual stress field induced by shot peening based on random-shots for 7075 aluminum alloy [J]. Transactions of Nonferrous Metals Society of China, 2012, 22(S): s261−s267.

[18] KAKIUCHI T, UEMATSU Y, HASEGAWA N, KONDOH E. Effect of ultrasonic shot peening on high cycle fatigue behavior in type 304 stainless steel at elevated temperature [J]. Journal of the Society of Materials Science Japan, 2016, 65(4): 325−330.

[19] DONG Zi-qiang, LIU Zhe, LI Ming, LUO Jing-li, CHEN Wei-xing, ZHENG Wen-xue, GUZONAS D. Effect of ultrasonic impact peening on the corrosion of ferritic–martensitic steels in supercritical water [J]. Journal of Nuclear Materials, 2015, 457: 266−272.

[20] XIAO Xu-dong, WANG Yong-jun, ZHANG Wei, WANG Jun-biao, WEI Sheng-min. Numerical simulation of stress peen forming with regular indentation [J]. Procedia Engineering, 2014, 81: 867−872.

[21] XIAO Xu-dong, WANG Yong-jun, ZHANG Wei, WANG Jun-biao, WEI Sheng-min. Numerical research on stress peen forming with prestressed regular model [J]. Journal of Materials Processing Technology, 2015, 229: 501−513.

[22] MIAO H Y, DEMERS D, LAROSE S, PERRONA C, MARTIN L. Experimental study of shot peening and stress peen forming [J]. Journal of Materials Processing Technology, 2010, 210: 2089−2102.

[23] HU Yong-xiang, LI Zhi, YU Xiong-chao, YAO Zhen-qiang. Effect of elastic prestress on the laser peen forming of aluminum alloy 2024-T351: Experiments and eigenstrain-based modeling [J]. Journal of Materials Processing Technology, 2015, 221: 214−224.

预应力超声喷丸参数对板材弯曲曲率及球面变形的影响

张 涛[1,2]，李 磊[1]，鲁世红[1]，章珈彬[1]，周 圳[1]，龚 海[2]

1. 南京航空航天大学 机电学院，南京 210016；
2. 中南大学 高性能复杂制造国家重点实验室，长沙 410083

摘　要：采用弹性预应力超声喷丸成形技术解决自由超声喷丸成形中板材弯曲变形不充分及出现大球面变形的问题。通过对弹性预应力超声喷丸成形过程进行理论分析，研究弹性预弯力矩对弯曲变形的影响。为了定量描述喷丸过程中球面变形程度，定义球面变形系数。开展自由喷丸和弹性预应力喷丸实验，分析两种喷丸方式的区别，并研究喷丸成形参数对板材成形曲率及球面变形系数的影响。结果表明，弦向喷丸轨迹有利于提高板材展向弯曲变形、同时减小球面变形系数。大预弯曲率能增大展向弯曲变形，同时减小弦向变形，从而显著减小球面变形系数。大撞针速度、小板厚及小偏置距离均有利于提高展向弯曲变形；在预应力喷丸成形过程中，大撞针速度有利于减小球面变形，而板厚及偏置距离的变化对球面变形系数影响很小。综上，在预应力喷丸成形过程中，预弯曲率及喷丸轨迹是最重要的两个影响参数。本研究可为大厚度翼板类零件的预应力超声喷丸成形过程参数优化提供指导。

关键词：预应力超声喷丸成形；成形曲率半径；球面变形系数

(Edited by Wei-ping CHEN)